Journal of Lasers, Optics & Photonics
ISSN: 2469-410X

Sudha et al., J Laser Opt Photonics 2018, 5:2
DOI: 10.4172/2469-410X.1000184

Research Article Open Access

Synthesis, Structural, Spectral, Optical and Mechanical Study of Benzimidazolium Phthalate crystals for NLO Applications

Sudha N[1], Abinaya B[1]*, Arun Kumar R[2] and Mathammal R[1]

[1]*Department of Physics, Sri Sarada College for Women (Autonomous), Salem, Tamil Nadu, India*
[2]*Department of Physics, PSG College of technology, Coimbatore, Tamil Nadu, India*

Abstract

Organic nonlinear crystal benzimidazolium phthalate have been grown by slow evaporation solution growth technique. The crystal belongs to orthorhombic crystal system space group P21. The functional groups present in the crystal were identified by FT-IR spectrum. The UV-Visible spectrum study reveals that the crystal has excellent transmittance the cut-off region being 205 nm. The photoluminescence spectrum shows violet emission. The chromaticity coordinates are calculated from the emission spectra and the emission intensity of the grown crystal is characterized through color chromaticity diagram. Dielectric studies find a way for the crystal to be used for opto electronic devices. Vicker's hardness test shows its mechanical behavior. The NLO property was confirmed by green emission in SHG test.

Keywords: Organic crystal; UV; FTIR; SHG; CIE

Introduction

In recent years, organic nonlinear optical crystals have been greatly investigated due to their high nonlinearities and rapid response in electro-optic effect compared to inorganic materials. The organic nonlinear optical crystals play an important role in electro-optic modulation, frequency mixing, second harmonic generation, optical parameter oscillation, high optical data storage telecommunication and optical information processing [1,2]. NLO crystals with proficient optical frequency conversion are the key elements for the development of laser systems, such systems are of colossal importance in tunable sources [3,4]. For such important application point of view, there is a great demand to synthesize new NLO materials with unique properties and to grow good quality single crystals. In recent years formation of salt or complex help in enhancing the nonlinearity of a material. Various materials like L-threonine phthalate, benzimidazole succinate, benzimidazole maelate, benzimidazole tartrate, benzimidazole fumarate benzimidazole isophthalate, benzimidazole teraphthalate, bezimidzolen hydroxybenzonic acid have been grown successfully for application point of view [5-8]. Hence an attempt has been made to grow Benzimidazolium phthalate for NLO applications, full structure of Benzimidazolium Phthalate have been solved by Martin and Craig Robert Leslie [8]. In this present investigation, we report the synthesis, structural, spectral, optical and mechanical properties of benzimidazolium phthalate

Experimental Procedure

Benzimidazolium phthalate (BPA) single crystal was grown by slow evaporation solution growth method. Benzimidazole and phthalic acid was used as a precursor material. As an initial step, the stoichiometric quantities of the primary materials, benzimidazole and phthalic acid were dissolved in ethanol separately. After mixing these core materials, the solution began to precipitate due to chemical formation. Double distilled water was added drop wise to the precipitate and the solution was stirred at 25°C when the precipitate got completely dissolved, it was stirred at room temperature for 5 hrs. The final solution was filtered using whatmann filter paper and allowed to evaporate at room temperature. The first nucleation peak was observed after 7 days. The crystal was formed after 15 days. As grown crystal of BPA is shown Figure 1. The typical size of the crystal was 11 mm × 4 mm × 3 mm. The crystal was found to be non-hygroscopic and highly stable (Tables 1 and 2).

Results and Discussion

X-ray diffraction analysis

The single crystal XRD analysis confirms that the grown crystal belongs to Orthorhombic crystal system with lattice parameter a=4.623 Aº, b=11.254 Aº and c=25.85 Aº having non centro symmetry space group $P2_12_12_1$ which is in good agreement with the reported values [8]. The reaction scheme shows that a proton has transferred from phthalic acid to Benzimidazole (Figures 2 and 3).

The result is the normalization of the internal bond lengths (N1-C1 1.321(6)Å, N2-C1 1.326(5)Å) and angles (C2-N1-C1 107.8(3)º, C7-N2-C1 107.9(3)º) and the creation of a positive charge that is delocalized over the 5-membered ring. Within the molecular complex the phthalic

Figure 1: As grown crystal of BPA by slow evaporation method.

***Corresponding author:** Abinaya B, Department of Physics, Sri Sarada College for Women (Autonomous), Salem, Tamil Nadu, India, Tel: 0427 244 7664; E-mail: abinayasmart20@gmail.com

Received April 06, 2018; **Accepted** May 17, 2018; **Published** May 24, 2018

Citation: Sudha N, Abinaya B, Arun Kumar R, Mathammal R (2018) Synthesis, Structural, Spectral, Optical and Mechanical Study of Benzimidazolium Phthalate crystals for NLO Applications. J Laser Opt Photonics 5: 184. doi: 10.4172/2469-410X.1000184

Crystal data	Present work	Reference work
a	4.613 A°,	4.623 A°,
b	11.222 A°	11.254 A°
c	25.77 A°	25.85 A°
α=β=γ	90˚,90˚,89.95˚	90˚, 90˚, 90˚
System	Orthorhombic	Orthorhombic
Space group	$P2_12_12_1$	$P2_12_12_1$

Table 1: Lattice parameters of BPA crystal.

Interaction	Length (Å) (D···A(Å))	For Hydrogen Bonds		
		D-H(Å)	H···A(Å)	D-H···A angle(°)
O2···O3	2.378(4)	1.179(3)	1.207(3)	170.6(2)
N1···O4	2.691(5)	1.001(3)	1.710(3)	165.7(2)
N2···O1	2.759(6)	1.000(3)	1.778(3)	165.0(2)
N2···O2	3.038(5)	1.000(3)	2.403(3)	120.7(2)
C4···O4	3.344(6)	0.909(5)	2.533(4)	148.9(3)
C10···O1	3.329(6)	0.943(4)	2.681(4)	126.5(3)
C5···π	3.847	-	-	-

Table 2: The three scalar quantities and bond angles of the hydrogen bonds and list of the interaction between the molecules in the benzimidazolium phthlate molecular complex.

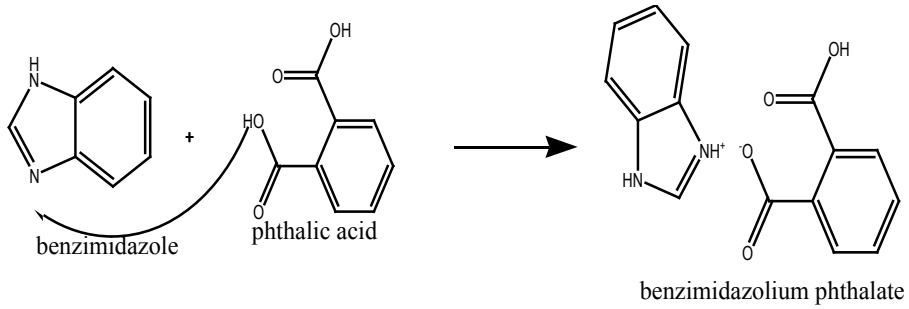

Figure 2: Reaction Scheme.

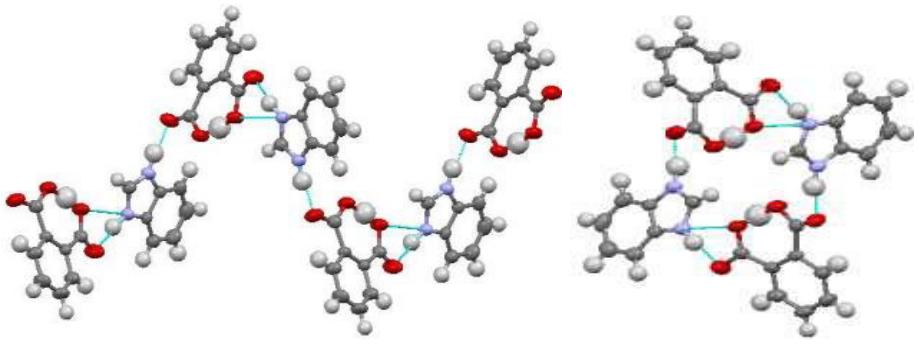

Figure 3: LHS, view of the main motif, linear chain of alternating hydrogen bonded co-molecules; RHS, view along the a-axis that highlights the spiral nature of the chain.

acid molecule is deprotonated, creating the phthlate species. Within this molecule an intramolecular hydrogen bond between the hydroxyl and carboxylate groups is formed, as in the other phthlate molecular complexes. The intermolecular hydrogen bond, O2-H-O3 is strong with an O-O distance of (2.398(2)Å). Which is consistent with the hydrogen bond found within the 2,6-dimethylpyridinium hydrogen phthalate molecular complex, (2.398(2)Å). The intramolecular hydrogen bond results in the proton being shared over the two oxygen's, this can be seen in the carbon-oxygen bond distances which have been slightly normalized, C1-O1 1.233(6)Å, C1-O2 1.275(5)Å, C8-O3 1.280(5)Å and C8-O4 1.243(6)Å. Due to charge transfer between the accepter and donor bridge the crystal can be used for NLO devices fabrication [8].

FT-IR spectral studies

Vibrational spectroscopy gives information on molecular vibration and their information is of immense help to organic chemist because it can be directly related to molecular structure [9]. To analyze the presence of functional group of BPA qualitatively, FT-IR Spectra was

recorded. The infrared assignments were made in the range from 400 cm^{-1} to 4000 cm^{-1} with the help of spectrum recorded on BRUKER IFS66/S spectrometer using KBr pellet technique. The recorded spectra were compared with the standard spectra of the functional group [10]. All the absorption frequencies and their tentative assignment are listed in Table 3 and Figure 4 shows the IR profile of BPA crystal. The standard assignments value of NH^+ bending vibration is 1650-1580 cm^{-1}, the BPA crystal observed at 1619 cm^{-1} [11]. The standard assignments value of aromatic C-H stretching vibration is 3100-3000 cm^{-1}, in BPA crystal peak at 3063 cm^{-1}, 3039 cm^{-1}, 3005 cm^{-1} is due to C-H stretching [12]. Generally C-C stretching vibrations are around 1625-1430 cm^{-1}, in the present compound peaks at 1458 cm^{-1}, 1477 cm^{-1} is due to C-C stretching. The standard assignments value of C-N stretching vibration is 1030-1600 cm^{-1} ,the BPA crystal occur in the region1133 cm^{-1}, 1201 cm^{-1}, 1245 cm^{-1}, 1363 cm^{-1}, 1409 cm^{-1}. The standard assignments value of C=O stretching vibration at 1850-1550 cm^{-1} the strong peak at 1771 cm^{-1} indicates the presence of C=O stretching in phthalic acid. The O-H bending in carboxylic acid occurs in the region 957 cm^{-1}, 1002 cm^{-1}. The standard assignment value of asymmetric COO^- stretching vibration is 1650-1400 cm^{-1}, in BPA the peak appeared at 1587 cm^{-1} [13] is due to COO^- stretching. The standard value of C-C out of plane is 600-420 cm^{-1} in the present compound the peak 542 cm^{-1} confirms C-C out of plane bending.

Assignment	Wave number cm^{-1}
NH^+ bending	1619
C-H stretching	3063,3039,3005
C-C stretching	1458,1477
C-N stretching	1133,1201,1245,1363,1409
C=O stretching	1771
O-H bending	957,1002
COO^- stretching	1587
C-O asymmetric stretching	1272,1302
C-C out of plane	542

Table 3: Assignment of IR band frequencies (cm^{-1}) observed for BPA crystal.

Optical transmission studies

To determine the transmission range UV-Vis-Nir spectrum was recorded using PERKIN ELMER LAMBDA 35 SPECTROMETER in the range 200-1200 nm covering entire near ultra violet region [14]. The obtained absorption and transmission spectrum is shown in Figure 5a, and 5b, respectively. The lower UV cut off wavelength is around 205 nm. The band gap is estimated using the formula, $E_g=1240/\lambda_{max}$ and it is found to be 4.57 eV [15]. The optical transmittance of the grown crystal clearly shows that the defects concentration is very less, which is favorable for linear optical window and NLO devices.

Photoluminescence spectra

The Photoluminescence intensity highly dependent on the crystallinity and structural perfection of the crystal. The Photoluminescence spectrum of the crystal was record using Perkin Elmer LS45 fluorescent spectrum. The emission spectrum was record between 270 nm to 800 nm shown in Figure 6. At the intense sharp emission peaks occur at 596 nm and 601 nm, owing to the emission of orange radiation. The strong PL emission of the material devices [16] and the sharp peak with high intensity confirms the high crystallinity of the sample.

CIE chromaticity coordinates

To characterize the true color emitted nature of the material, it is necessary to study the color coordinates marked on a standard chromaticity diagram [17]. The CIE 1931 (Commission International d'Eclairage) diagram is a universal method to represent all the possible colors by combining three primary colors and is used to quantify

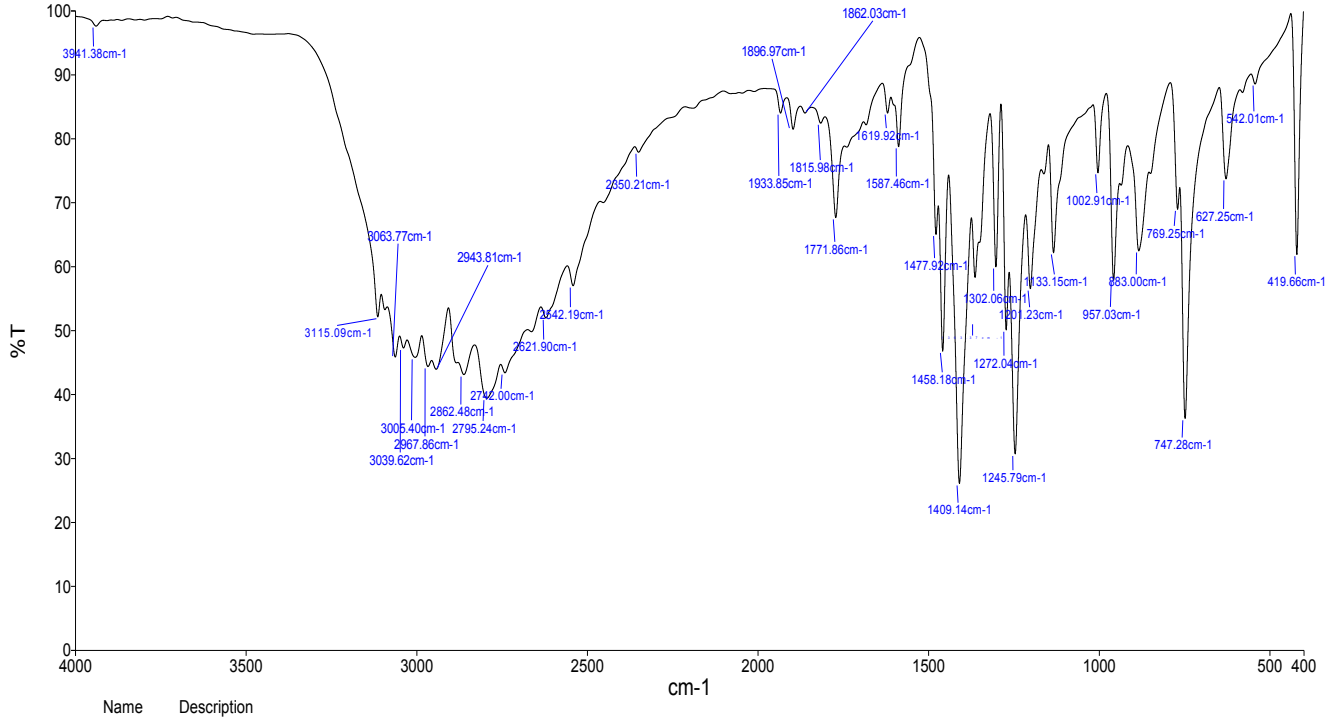

Figure 4: FTIR spectrum of BPA crystal.

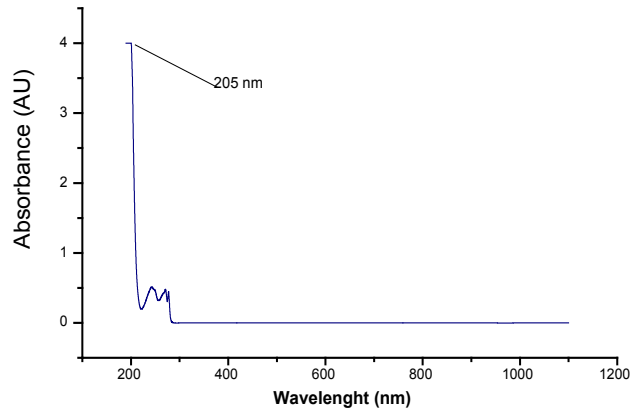

Figure 5a: UV – Vis – NIR Absorbance Spectrum.

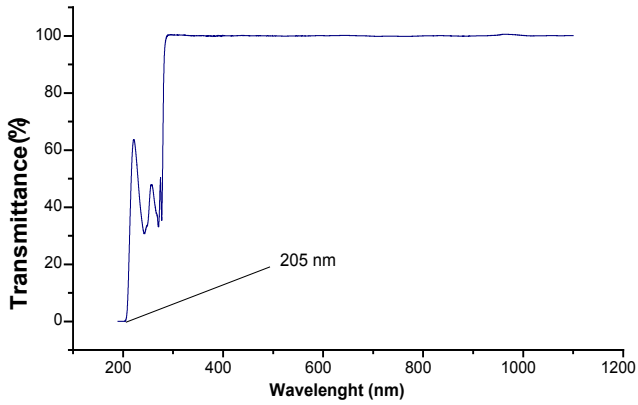

Figure 5b: UV – Vis – NIR Transmittance Spectrum.

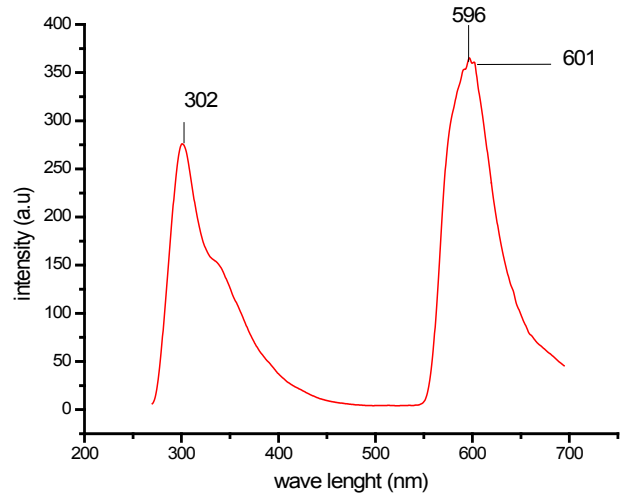

Figure 6: Fluorescence spectrum of BPA Crystal.

the tun ability of emission wavelength and the change in intensity of the emission band. The emission intensities of the BPA crystals are characterized through a CIE 1931 color chromaticity diagram. Three color matching functions such as $\bar{x}(\lambda)$, $\bar{y}(\lambda)$, and $\bar{z}(\lambda)$ provide enough description of the color produced by any light source. The real spectral colors can be obtained by adding three artificial 'colors' denoted as X, Y, and Z called the tristimulus values. The degree of stimulation necessary to match the color of a given power spectral density $P(\lambda)$ can be expressed as [18]

$$X = \int \bar{x}(\lambda)P(\lambda)d\lambda,$$

$$Y = \int \bar{y}(\lambda)P(\lambda)d\lambda,$$

$$Z = \int \bar{z}(\lambda)P(\lambda)d\lambda$$

where X, Y, and Z are the tristimulus values and give the power for each of the three primary colors required to match with the color of $P(\lambda)$. From these tristimulus values, the color chromaticity coordinates x and y can be determined from the following expression [19]

$$x = \frac{X}{X+Y+Z},$$

$$y = \frac{Y}{X+Y+Z}$$

The calculated (x, y) coordinates are found to be (0.574369, 0.389454) corresponding to the grown crystal. The location of the chromaticity coordinates (x, y) of the crystal is shown in Figure 7. It is evident from the figure that the color co-ordinates of BPA crystals fall in the orange region of the CIE-1931 chromaticity diagram under the 302 nm wavelength excitation [20].

Micro hardness studies

Quality crystal with good optical performance and excellent mechanical behavior are required for various industry applications. To study the mechanical behavior of the crystal micro hardness studies have been carried out on the grown crystal using SHIMADZU micro hardness tester, fitted with diamond Vicker's Pyramidal indenter. The well-polished crystal was placed on the platform of vicker's hardness tester and the loads with different magnitudes were applied in a fixed interval of time. The indentation time was kept as 10 s for the entire load. Vicker's hardness value have be calculated using the formula

$$\mathbf{H_v = 1.854 \times P/d^2\ Kg/mm^2}$$

where $\mathbf{H_v}$ Vicker's micro hardness number, **P** applied load in Kg and **d** mean Diagonal length of indentation (mm). The trace of Vicker's hardness number with various load shown in Figure 8a which shows that the hardness increase with increase of load up of 100 g. Microhardness testing is one of the best methods of understanding the

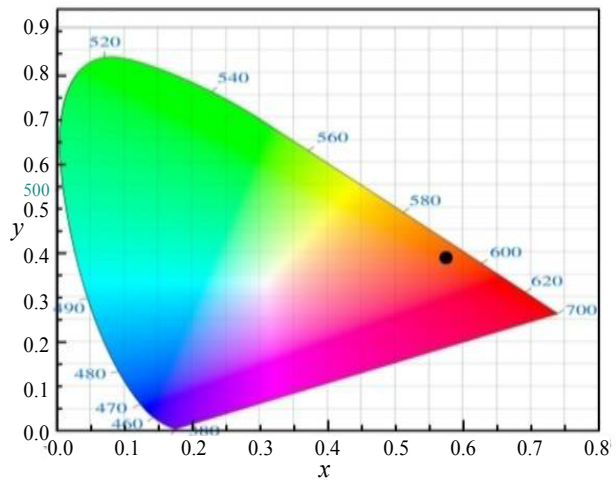

Figure 7: CIE color chromaticity diagram of BPA crystal.

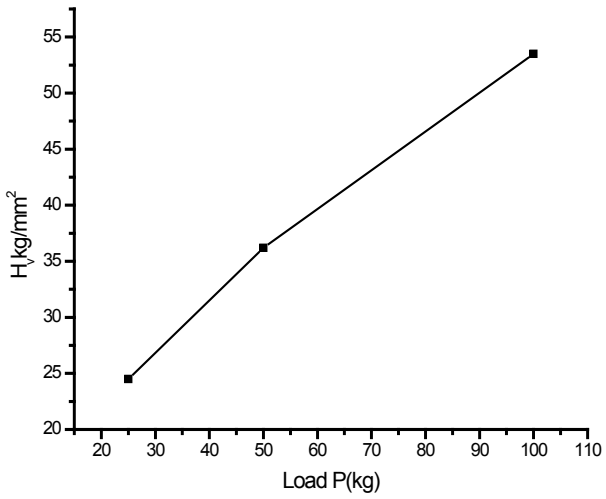

Figure 8a: Hardness Vs load graph.

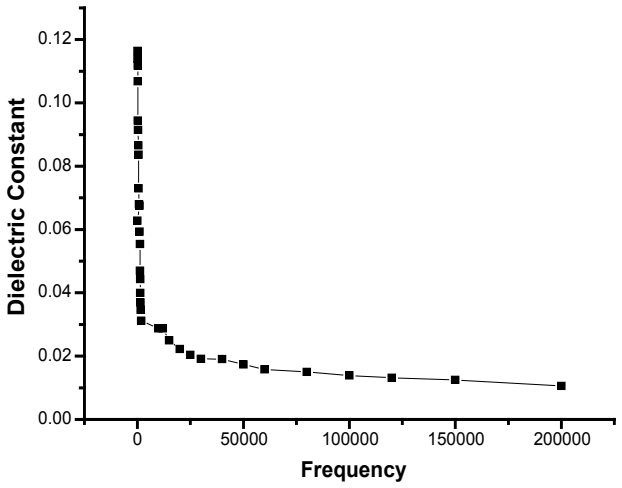

Figure 9a: Variation of dielectric constant with frequency.

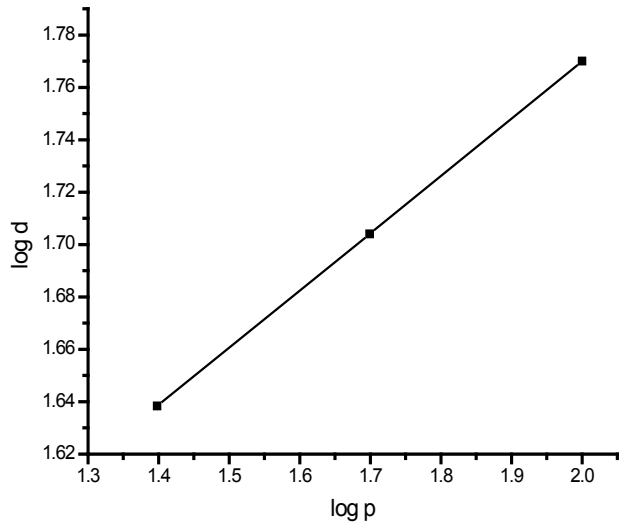

Figure 8b: log p Vs log d graph.

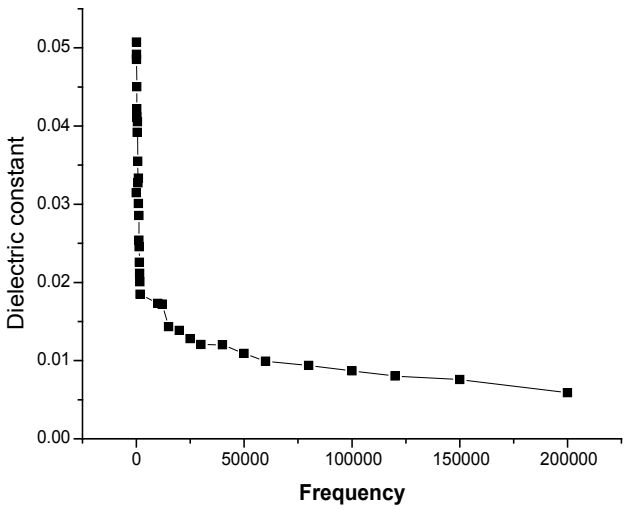

Figure 9b: Variation of dielectric loss with frequency.

mechanical property of the material such as fracture behavior, yield strength, brittleness index and temperature [20,21]. The ratio between the load and size of indentation is given by Mayer's law [22] as

$$P=ad^n$$

Where **P** is the load (g), **d** is the diameter of indentation (mm), **a** and **n** are constants for a given material. By plotting log P verses log d. Figure 8b shows the value of the work hardening co-efficient n was found to be 1.6. According to Onitsch, $1.0 \leq n \leq 1.6$ for hard material and n>1.6 for soft material [23]. The value of the working hardening co-efficient n was founded to be 2. Hence it is concluded that BPA crystal belongs to the soft material category.

Dielectric studies

Dielectric constant: The dielectric constant of the BPA crystal it studied at room temperature using digital LCRZ meter in the frequency region from 50 Hz to 200 KHz. The dielectric analysis is an essential characteristic that can be used to get information based on the electrical properties of the material as a Figure 9a shows that the dielectric constant decrease with frequency reveals the material can be enhance for second harmonic generation [24-28].

Dielectric loss: The dielectric loss is inversely proportional shown in Figure 9b. In accordance with Miller rule, the lower value of dielectric constant at higher frequencies is a suitable parameter for the enhancement of SHG coefficient [29]. The low value of dielectric loss at high frequency reveals the high optical quality of the crystal with lesser defects and optical quality which can be used for device fabrication [30]. Thus, the low value of dielectric constant and dielectric loss at higher frequencies is important for extending towards, photonic, electro-optic devices.

Non linear optical study

Kurtz Perry powder technique is a valuable tool to elucidate the second harmonic generation of a material. The powder SHG efficiency

of BPA crystal was determined using Kurtz and Perry Powder technique [31]. Its enables to measure the SHG efficiency of a material relative to standard urea. A Q-switched Nd:YAG laser operating at 1064 nm and 8 ns pulse width with an input repetition rate of 10 Hz and energy 1.2 mj/pulse. The second harmonic signal generated in the crystalline sample was confirmed from the emission of green radiation of wavelength 532 nm from the crystalline. The SHG output was converted into electronic signal and was displaced on a digital storage oscilloscope from the obtained data it is found that the input voltage is 1.2 mJ/pulse and output for BPA and standard urea is 17.60 mV and 52 mV, respectively. The SHG efficiency of BPA sample is 0.3 times than that well known standard urea. This conforms BPA can be used for NLO applications.

Conclusion

Optically good quality Benzimidazolium phthalate crystals were grown by slow evaporation technique. The single XRD studies reveal that BPA belongs to orthorhombic system. The presence of functional group was confirmed by FT-IR spectra. The UV-Vis studies reveal that the crystal is transparent in the entire region with a UV-Vis region cut-off being 205 nm. The PL and CIE chromaticity diagram nominate the crystal for orange emission region. The mechanical behavior has been studied by Vicker's hardness test. The low dielectric constant and dielectric loss at high frequency region also suggest that BPA can be used for optoelectronic devices. The second harmonic generation property was tested using Kurtz and Perry technique and founded 0.3 times that of urea. Owing to all these properties BPA crystals could be a promising material for the nonlinear optical applications.

Acknowledgements

The authors are also thankful to Prof. Das PK Department of Inorganic and Physical Chemistry IISc Bangalore for extending SHG measurement, St. Joseph's College Trichirappalli for providing spectral measurement, Sophisticated Analytical Instrumentation Facility (SAIF), IIT Chennai for XRD measurements and Prof Dr. Arun Kumar R, Department of Physics PSG College of Technology, Coimbatore for providing CIE chromaticity diagram.

References

1. Chemla DS, Zyss J (1987) Nonlinear Optical Properties of Organic Molecules and Crystals, Academic Press, London Volume: 1.
2. Badan J, Hierle R, Perigand A, Zyss J, (1993) Nonlinear Optical Properties of Organic Molecules and Polymeric Materials. Am Chem.Soc, USA 233: D5.
3. Packiya raj M, Ravi Kumar SM, Sivavishnu D, Kubendiran T, Anbarasi A, et al. Synthesis, Growth and Optical, Mechanical, Electrical and Surface Properties of an inorganic new nonlinear optical crystal: sodium cadmium tetra chloride (sctc). Cryst Res Technol.
4. Iwai M, Kobayashi T, Furya H, Mori Y, Sasaki T (1997) Jpn J Appl Phys 36: 276-279.
5. Zyss J, Nicoud JF, Coquillay M (1984) Chirality and hydrogen bonding in molecular crystals for phase-matched second-harmonic generation: N-(4-nitrophenyl)-(L)-prolinol (NPP). J Chem Phys 81: 4160-4167.
6. Ledoux I, Badan J, Zyss J, Migus A, Hulin D (1987) Generation of high-peak-power tunable infrared femtosecond pulses in an organic crystal: application to time resolution of weak infrared signals. J Opt Soc Am B 4: 987–997.
7. Mallik T, Kar T, Bocelli G, Musatti A (2006) Structural and thermal characterization of L-arginine dihydrate - a nonlinear optical material. Cryst Res Technol 41: 280-284.
8. http://theses.gla.ac.uk/3154/
9. Mohan J (2014) Organic Spectroscopy: Principle And Applications. Alpha Science International Ltd 204: 8.
10. Scorates G (2011) Infrared and raman charatersticies group frequencies: Tables and Charts, 3rd Edition John Wiley & sons LTD, pp: 155-159.
11. Britto Dhas SAM, Suresh M, Bhavannarayana G, Natarajan S (2008) Growth and characterization of a new potential NLO material from the amino acid family—L-prolinium picrate. J Crst Growth 310: 3535-3539.
12. Leela S, Hema R, Stoeckil-Evans H, Ramamurthi K, Bhavannarayana G (2010) Design, synthesis, growth and characterization of 4-methoxy-4′-dimethylamino-benzylidene aniline (MDMABA): A novel third order nonlinear optical material. Spectrochim, Acta A: Mol Biomol, Spectrosc 77: 927-932.
13. Vimala M, Rajesh Kumar T, Tamilselvan S, Sagayaraj P, Mahadevan CK (2010) Growth and properties of novel organic nonlinear optical crystal: l-alaninium tartrate (LAT). Physica B 405: 3907-3913.
14. Jiang H, Fang Q (1999) Organic and Semiorganic Nonlinear Optical Materials. Advanced Material 13: 1147-1151.
15. Selvarajn P, Glorium Arul Raj J, Perumal S, (2009) Characterization Of Pure And Urea Doped γ-Glycine.Single Crystal Grown By Solution Method. J Crystal growth 333: 3835-3840.
16. Kasap S, Capper P, (2006) Springer Handbook of Electronics and Photonic Material. Springer Science Inc PP: 983-996.
17. Gao SP, Qian YN, Wang B (2015) Photoluminescence of rare-earth ion (Eu3+, Tm3+, and Er3+)-doped and co-doped ZnNb2O6 for solar cells. Chin Phys 24: 087803.18.
18. Kumar JS, Pavani K, Babu AM, Giri NK, Rai SB, et al. (2010) Fluorescence characteristics of Dy3+ ions in calcium fluoroborate glasses. J Lumin 130: 1916-1923.
19. Lawn BR, Fuller ER (2016) Equilibrium Penny-Like Crack in Indentation Fracture. J Mater Sci Lett 75:10.
20. Kumaresh A, Arun Kumar R, Ravikumar N, Madhusoodana U, Panigrahi BS, et al. (2016) Structural and photoluminescence studies on europium-doped lithium tetraborate (Eu:Li2B4O7) single crystal grown by microtube Czochralski (μT-Cz) technique*. Chin Phys 25: 5.
21. Brook W, Flow JH (1958) In Rock Salt Structure Report 58-RI, 2033 of GE Research Laboratory USA.
22. Reyes H, Muñoz,a MB, Farfán N, Santillan R, Rojas-Lima S, et al. (2002) Synthesis, crystal structures, and quadratic nonlinear optical properties in a series of push–pull boronate derivatives. Mater Che 12: 2898- 2903.
23. Onitsch EM (1947) Mikroscopia 2: 131.
24. Aakeroy CB, Seddon KR (1993) The hydrogen bond and crystal engineering. Chem Soc Rev 22: 397-407.
25. Aakeroy CB (1997) Crystal Engineering: Strategies and Architectures. Acta Cryst B 53: 596-586.
26. Rrychlewska U, Warajtis R (2000) Packing modes of (R,R)-tartaric acid esters and amides. Acta Cryst B 56: 833-848.
27. Rrychlewska U (1994) J Mol Struc 474: 569-586.
28. Rajesh K, Miltonboaz B, Kumar P (2013) Growth and Characterization of Pure and Doped L-Alanine Tartrate Single Crystals. Journal of Material 21: 1-5.
29. Hundelshausen VU (1971) Electrooptic effect and dielectric properties of cadmium-mercury-thiocyanate crystals. Phys Lett 34: 405-406.
30. Balarew C, Duhlew R (1984) Application of the hard and soft acids and bases concept to explain ligand coordination in double salt structures. J Solid State Chem 55: 1-6.
31. Kurtz SK, Perry TT (1968) A Powder Technique For The Evaluation Of Non Linear Optical Material. J Phys D Appl Phys 39: 3798-3813.